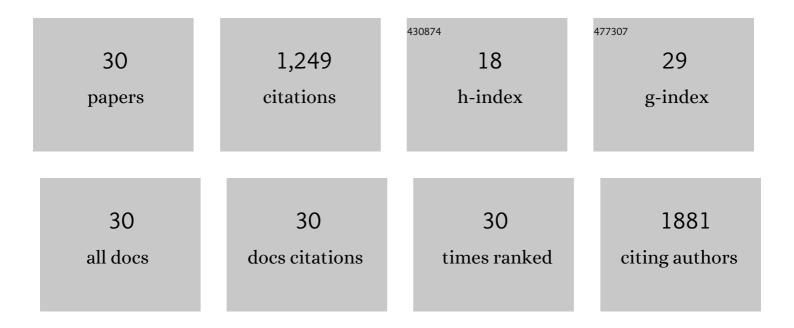
## Murray C Richardson

List of Publications by Year in descending order

Source: https://exaly.com/author-pdf/9202165/publications.pdf Version: 2024-02-01



#	Article	IF	CITATIONS
1	Diet influences on growth and mercury concentrations of two salmonid species from lakes in the eastern Canadian Arctic. Environmental Pollution, 2021, 268, 115820.	7.5	10
2	Hydrologic control on winter dissolved oxygen mediates arsenic cycling in a small subarctic lake. Limnology and Oceanography, 2021, 66, S30.	3.1	18
3	Mercury concentrations and associations with dissolved organic matter are modified by water residence time in eastern Canadian lakes along a 30° latitudinal gradient. Limnology and Oceanography, 2021, 66, S64.	3.1	10
4	Mineralogical, geospatial, and statistical methods combined to estimate geochemical background of arsenic in soils for an area impacted by legacy mining pollution. Science of the Total Environment, 2021, 776, 145926.	8.0	16
5	Wetlands and lowâ€gradient topography are associated with longer hydrologic transit times in Precambrian Shield headwater catchments. Hydrological Processes, 2020, 34, 598-614.	2.6	15
6	Seasonal variation of arsenic and antimony in surface waters of small subarctic lakes impacted by legacy mining pollution near Yellowknife, NT, Canada. Science of the Total Environment, 2019, 684, 326-339.	8.0	53
7	The role of wetland coverage within the nearâ€stream zone in predicting of seasonal stream export chemistry from forested headwater catchments. Hydrological Processes, 2019, 33, 1465-1475.	2.6	27
8	Environmental Drivers of Rare Earth Element Bioaccumulation in Freshwater Zooplankton. Environmental Science & Technology, 2019, 53, 1650-1660.	10.0	26
9	Quantifying the relative contributions of vegetation and soil moisture conditions to polarimetric C-Band SAR response in a temperate peatland. Remote Sensing of Environment, 2018, 206, 123-138.	11.0	46
10	Ratio of Methylmercury to Dissolved Organic Carbon in Water Explains Methylmercury Bioaccumulation Across a Latitudinal Gradient from North-Temperate to Arctic Lakes. Environmental Science & Technology, 2018, 52, 79-88.	10.0	28
11	Soil Moisture Monitoring in a Temperate Peatland Using Multi-Sensor Remote Sensing and Linear Mixed Effects. Remote Sensing, 2018, 10, 903.	4.0	11
12	The impacts of environmental variables on water reflectance measured using a lightweight unmanned aerial vehicle (UAV)-based spectrometer system. ISPRS Journal of Photogrammetry and Remote Sensing, 2017, 130, 217-230.	11.1	70
13	Delineation of peatland lagg boundaries from airborne LiDAR. Journal of Geophysical Research G: Biogeosciences, 2017, 122, 2191-2205.	3.0	9
14	Random forests as cumulative effects models: A case study of lakes and rivers in Muskoka, Canada. Journal of Environmental Management, 2017, 201, 407-424.	7.8	21
15	A Systematic Approach for Variable Selection With Random Forests: Achieving Stable Variable Importance Values. IEEE Geoscience and Remote Sensing Letters, 2017, 14, 1988-1992.	3.1	80
16	Moving to the RADARSAT Constellation Mission: Comparing Synthesized Compact Polarimetry and Dual Polarimetry Data with Fully Polarimetric RADARSAT-2 Data for Image Classification of Peatlands. Remote Sensing, 2017, 9, 573.	4.0	41
17	Fusion of Multispectral Imagery and Spectrometer Data in UAV Remote Sensing. Remote Sensing, 2017, 9, 696.	4.0	28
18	Empirical assessment of effects of urbanization on event flow hydrology in watersheds of Canada's Great Lakes-St Lawrence basin. Journal of Hydrology, 2016, 541, 1456-1474.	5.4	21

2

MURRAY C RICHARDSON

#	Article	IF	CITATIONS
19	Change in event-scale hydrologic response in two urbanizing watersheds of the Great Lakes St Lawrence Basin 1969–2010. Journal of Hydrology, 2015, 527, 1174-1188.	5.4	9
20	On the Importance of Training Data Sample Selection in Random Forest Image Classification: A Case Study in Peatland Ecosystem Mapping. Remote Sensing, 2015, 7, 8489-8515.	4.0	398
21	Assessing the Potential to Operationalize Shoreline Sensitivity Mapping: Classifying Multiple Wide Fine Quadrature Polarized RADARSAT-2 and Landsat 5 Scenes with a Single Random Forest Model. Remote Sensing, 2015, 7, 13528-13563.	4.0	20
22	Wetland mapping with LiDAR derivatives, SAR polarimetric decompositions, and LiDAR–SAR fusion using a random forest classifier. Canadian Journal of Remote Sensing, 2013, 39, 290-307.	2.4	107
23	The influence of hyporheic exchange on reachâ€scale water budgets in a Precambrian Shield catchment, Quebec, Canada. Hydrological Processes, 2013, 27, 1890-1900.	2.6	Ο
24	The role of terrestrial vegetation in atmospheric Hg deposition: Pools and fluxes of spike and ambient Hg from the METAALICUS experiment. Global Biogeochemical Cycles, 2012, 26, .	4.9	45
25	Contributions of streamflow variability, concentration–discharge shifts and forested wetlands to terrestrial–aquatic solute export in Precambrian Shield headwater catchments. Ecohydrology, 2012, 5, 596-612.	2.4	16
26	The influences of catchment geomorphology and scale on runoff generation in a northern peatland complex. Hydrological Processes, 2012, 26, 1805-1817.	2.6	18
27	Areal differentiation of snow accumulation and melt between peatland types in the James Bay Lowland. Hydrological Processes, 2012, 26, 2663-2671.	2.6	6
28	Water storage dynamics and runoff response of a boreal Shield headwater catchment. Hydrological Processes, 2011, 25, 3042-3060.	2.6	46
29	Analysis of airborne LiDAR surveys to quantify the characteristic morphologies of northern forested wetlands. Journal of Geophysical Research, 2010, 115, .	3.3	29
30	Hydrogeomorphic edge detection and delineation of landscape functional units from lidar digital elevation models. Water Resources Research, 2009, 45, .	4.2	25